frontiers in Pharmacology

ORIGINAL RESEARCH
published: 04 March 2022
doi: 10.3389/fphar.2021.811331

Comprehensive Metabolomics and Network Pharmacology to Explore the Mechanism of 5-Hydroxymethyl Furfural in the Treatment of Blood Deficiency Syndrome

Wensen Zhang[1†], Na Cui[1†], Fazhi Su[1], Yangyang Wang[1], Bingyou Yang[1], Yanping Sun[1], Wei Guan[1], Haixue Kuang[1] and Qiuhong Wang[2]**

[1]Key Laboratory of Basic and Application Research of Beiyao (Heilongjiang University of Chinese Medicine), Ministry of Education, Harbin, China, [2]School of Traditional Chinese Medicine, Guangdong Pharmaceutical University, Guangdong, China

Radix Rehmanniae (RR, from Radix Rehmanniae (Gaertn.) DC.) is a natural medicine used in traditional Chinese medicine (TCM) since ancient times for the treatment of blood disorders. RR is steamed to get Rehmanniae Radix Praeparata (RP), which has a tonic effect on blood; the content of 5-hydromethylfurfural (5-HMF) increases more than four times after steaming. Studies have shown that 5-HMF has positive pharmacological effects on cardiovascular and hematological disorders. This study aimed to explore and verify the impact of 5-HMF on rats with chemotherapy-induced blood deficiency syndrome (BDS). Rats were given cyclophosphamide (CP) and acetophenhydrazine (APH) to induce BDS, the coefficients of some organs (liver, spleen, and kidney) were measured, and a routine blood test examined the coefficients of several peripheral blood cells. Metabolomics and network pharmacology were combined to find important biomarkers, targets, and pathways. Western blot was used to detect the expression of CYP17A1 and HSD3B1 proteins in the spleen. All these findings suggested that the 5-HMF significantly increased the number of peripheral blood cells and reversed splenomegaly in rats. In addition, 5-HMF upregulated CYP17A1 and HSD3B1 protein expression in splenic tissues. Also, 5-HMF ameliorated chemotherapy-induced BDS in rats, and its therapeutic mechanism might depend on steroid hormone biosynthesis and other pathways. It acts on blood deficiency via multiple targets and pathways, which is unique to Chinese medicine.

Keywords: 5-HMF, blood deficiency, network pharmacology, metabolomics, Radix Rehmanniae

Abbreviations: SD, Standard deviation; EDTA, Ethylenediaminetetraacetic acid; TCMSP, Traditional Chinese Medicine Systems Pharmacology Database and Analysis Platform; OMIM, Online Mendelian Inheritance in Man; KEGG, Kyoto Encyclopedia of Genes and Genomes; GO, Gene Ontology; VIP, Variable importance in the projection.

OPEN ACCESS

Edited by:
Ren-ai Xu,
First Affiliated Hospital of Wenzhou Medical University, China

Reviewed by:
Shun-bin Luo,
Lishui City People's Hospital, China
Fangbo Xia,
University of Macau, China
Meichen Liu,
Chengdu University of Traditional Chinese Medicine, China

****Correspondence:***
Haixue Kuang
hxkuang@hljucm.net
Qiuhong Wang
qhwang668@sina.com

[†]These authors have contributed equally to this work

Specialty section:
This article was submitted to Drug Metabolism and Transport, a section of the journal Frontiers in Pharmacology

Received: *08 November 2021*
Accepted: *27 December 2021*
Published: *04 March 2022*

Citation:
Zhang W, Cui N, Su F, Wang Y, Yang B, Sun Y, Guan W, Kuang H and Wang Q (2022) Comprehensive Metabolomics and Network Pharmacology to Explore the Mechanism of 5-Hydroxymethyl Furfural in the Treatment of Blood Deficiency Syndrome. Front. Pharmacol. 12:811331. doi: 10.3389/fphar.2021.811331

1 INTRODUCTION

According to the theory of traditional Chinese medicine (TCM), blood deficiency is a common disease and a pathological state of blood dysfunction and organ malnutrition (Li et al., 2015). Blood deficiency syndrome (BDS) is mainly related to excessive blood loss (Shi et al., 2014), deficient spleen and stomach function, insufficient hematogenesis, and blood stasis (Yong et al., 2012). The main diagnostic index is the decrease in blood cells or hemoglobin content, similar to anemia (Wang et al., 2013). Modern medicine holds that patients with BDS often have clinical manifestations such as impaired hematopoietic function, decreased visceral function, malnutrition, and bone marrow suppression (Zhang et al., 2014). BDS can cause spleen enlargement (Zhang et al., 2020). After chemotherapy, most patients have a hemoglobin synthesis disorder, which causes BDS and severely interferes with blood system circulation (Jiang et al., 2013). However, anemia is defined only as a decrease in the concentration of hemoglobin in the body, which is usually related to a reduction in red blood cells (Li et al., 2017).During cancer treatment, the standard treatment for BDS is iron and vitamin B12 supplementation to promote the synthesis of erythropoietin, which can accelerate the recovery of the hematopoietic system (Brown 2020). However, the application of these regimens is limited because of their unstable efficacy, high cost, and side effects (Milano and Schneider 2007).

A main component of TCM is 5-HMF, among which the most representative herb is Rehmanniae Radix Praeparata (RP) (Won et al., 2014). Rehmanniae Radix (RR) is steamed to obtain RP, which is a plant of the Scrophulariaceae family. RP has been used to treat BDS for thousands of years. It is a commonly used TCM in Asia (Li et al., 2021). The Compendium of Materia Medica records that RP is used as a blood tonic (Guo et al., 2016), which regulates and fortifies blood and treats BDS (Zee-Cheng 1992). The main components of RR are monosaccharides, oligosaccharides (Kitagawa et al., 1995), iridoids (Xia et al., 2020), and glycosides (Xu et al., 2012). The decomposition products of these compounds constitute RP, of which 5-HMF is the most prominent (Won et al., 2014). During the processing of RR, stachyose is reduced to hexose, and these components finally form 5-HMF, which increases the content of 5-HMF in RP after steaming by more than four times compared with RR (Zhu et al., 2007). Therefore, 5-HMF has become the main active component of RP and is used as a marker compound for quality control (Li et al., 2005; Korean Food and Drug Administration, 2008). This transformation of active ingredients in raw materials and processed products leads to differences in their efficacy. For example, RP is better at supplementing blood (Xia et al., 2020). According to current research results, 5-HMF has positive pharmacological effects on cardiovascular and blood diseases. For example, 5-HMF can increase hemoglobin's oxygen affinity to support cardiac function during severe hypoxia (Lucas et al., 2019). It also has sound biological effects, such as antioxidant activity (Li et al., 2011) and strengthening the resistance of sickle red blood cells to injury caused by hypoxia (Qiang et al., 2021). Therefore, we speculate that 5-HMF can be used as a potential therapeutic drug for BDS. However, the treatment of BDS by 5-HMF has not been documented, and its therapeutic mechanism is unclear.

Network pharmacology and metabolomics are practical tools for elucidating the underlying mechanisms of TCM (Pan et al., 2020). First, a blood deficiency rat model induced by chemotherapy was used to evaluate the effect of 5-HMF on BDS. Second, a network pharmacology method was established to explore the mechanism of 5-HMF in treating BDS from the perspective of targets and pathways. At the same time, plasma metabolomics revealed the synergistic metabolic mechanism of metabolites and metabolic pathways. Finally, Western blot validated the metabolic pathway. This study was the first to use a combination of network pharmacology and plasma metabolomics to determine the mechanism of 5-HMF in the treatment of BDS. Hopefully, these results will provide a theoretical basis for elucidating the mechanism of 5-HMF in BDS treatment.

2 MATERIALS AND METHODS

2.1 Animals and Ethic Statement

We used 40 healthy male SD rats weighing 220–260 g, batch number SCXK (Liao) 2020–0001, from Liaoning Changsheng Biotechnology Co., Ltd. The animal experiment was approved by the Ethics Committee of Heilongjiang University of Traditional Chinese Medicine (approval number 2019121101). Animals were kept in a room at 25 C and 40–60% humidity. Rats were randomly divided into five groups with 8 rats in each group: control group, model group, 5-HMF-L group, 5-HMF-M group, and 5-HMF-H group.

2.2 Chemicals and Reagents

The 5-HMF was purchased from Aladdin (batch number H2020020, >95% (Gas chromatography), containing 3–5% water as a stabilizer). N-acetophenazine was purchased from Aladdin (batch number L1909182), and cyclophosphamide (CP) was purchased from MACKLIN (batch number C11147187).

2.3 Establishment of the Blood Deficiency Syndrome Model

The establishment of the BDS animal model was consistent with previous studies (Li et al., 2015). APH (20 mg/kg, 10 mg/kg) was injected subcutaneously on the first and fourth days. On the 4th day, 2 h after subcutaneous injection of APH, CP (20 mg/kg) was injected intraperitoneally. CP was injected for 4 consecutive days after that. On the 7th day, the indexes of red blood cells (RBC), white blood cells (WBC), hemoglobin (HGB), and hematocrit (HCT) in peripheral blood were measured. The control group was injected with the same volume of saline in the same way. From the first day, the treatment group was given 5-HMF (5.19 mg/kg, 2.595 mg/kg, 1.2975 mg/kg) by gavage (Duan 2021), respectively, and the control group and model group were given the same volume of saline by gavage for 15 days.

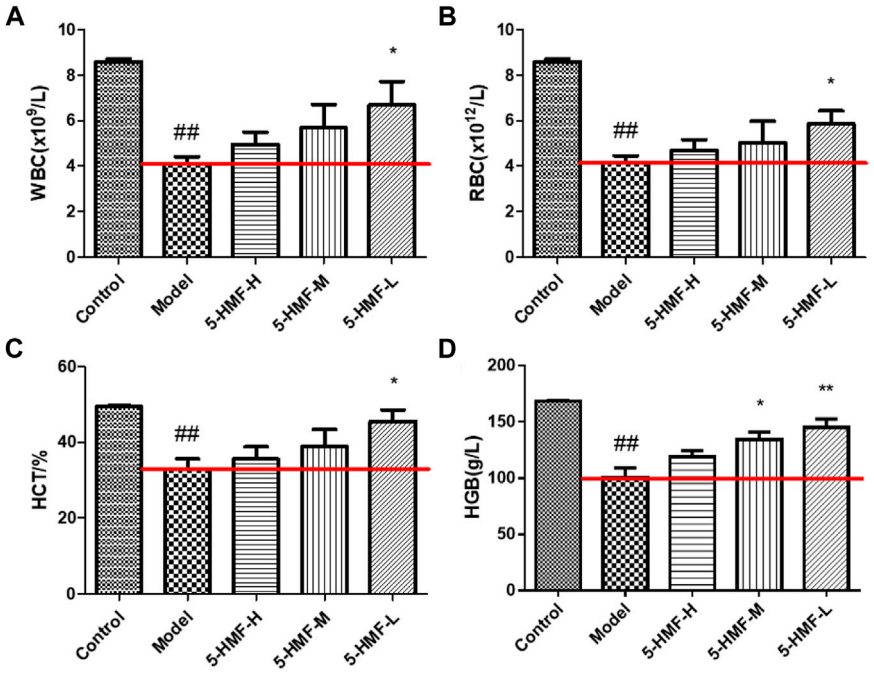

FIGURE 1 | The blood parameters of rats in the control and model groups treated with saline and different doses of 5-HMF. **(A)** The level of WBC. **(B)** The level of RBC. **(C)** The level of HGB. **(D)** The level of HCT. Each value represents the mean SD ($n = 8$); $^{\#}p < 0.05$ and $^{\#\#}p < 0.01$, compared with the control group; $^{*}p < 0.05$ and $^{**}p < 0.01$, compared with the model group.

2.4 Routine Blood Test

After the last administration, blood was taken from the abdominal aorta and collected in a sterile vacuum blood collection tube containing ethylenediaminetetraacetic acid (EDTA). The blood was analyzed by the HEMAVET 950 automatic hematology analyzer (Drew Scientific Group, Dallas, Texas, United States) to quantify RBC, WBC, HGB, and HCT.

2.5 Network Analysis

2.5.1 Target Prediction

The targets of 5-HMF were predicted in the following ways: Traditional Chinese Medicine Systems Pharmacology Database and Analysis Platform (TCMSP) (Ru et al., 2014), Swiss Target Prediction (Gfeller et al., 2014), Targetnet (Yao et al., 2016), PharmMapper (Wang et al., 2017). We used GeneCards (Stelzer et al., 2016), Online Mendelian Inheritance in Man (OMIM) (Amberger et al., 2015), Drugbank (Wishart et al., 2018) to identify targets related to BDS. In the OMIM database, we opened the Gene Map and entered "blood deficiency syndrome" to obtain 532 essential genes. We entered "blood deficiency syndrome" in the GeneCard database, selected genes with a relevance score >20, and obtained a total of 1,542 critical genes. We entered "anemia" in the Drugbank database and got a total of 11 essential genes and then removed the duplicated genes.

2.5.2 Kyoto Encyclopedia of Genes and Genomes and Gene Ontology Enrichment Analysis

In analyzing the common targets of the 5-HMF action target and BDS-related targets, the server Metascape (Zhou et al., 2019) was used for Kyoto Encyclopedia of Genes and Genomes (KEGG) and Gene Ontology (GO) enrichment analysis.

2.5.3 Network Construction

Two visualization networks were constructed: 1) Target point network, a network composed of 5-HMF, BDS, and common targets; 2) Targetpath network, in which the targets and their pathways were used to generate spatiotemporal networks. All networks were constructed by Cytoscape 3.8.0 (Liu et al., 2020).

2.6 LC-MS Metabolomics Analysis

2.6.1 Sample Preparation

After the final administration, the blood of rats was collected from the abdominal aorta, left to stand for 30 min at 4 C, centrifuged at 3,500 rpm/min for 15 min. Then the plasma supernatant sample was mixed 1:3 with acetonitrile, vortexed for 30 s, and left to stand for 30 min at −20°C. The blood was centrifuged at 13,500 rpm/min for 15 min at 4 C, 300 μL of supernatant was evaporated, and 150 μL of 50% acetonitrile was added to redissolve the sample. After centrifugation, the sample was injected into the injection cup for testing (Gong et al., 2019).

2.6.2 UPLC-QTOF/MS Analysis

The G2-Si (Waters Q-TOF SYNAPT from Manchester Waters Company) has a continuous mode and is equipped with an electrospray ion source. The plasma samples were chromatographed on an Acquity UPLC HSS T3 column with a gradient elution program at the flow rate of 0.2 μL/min. The mobile phase was comprised of water and 0.1% formic acid (phase

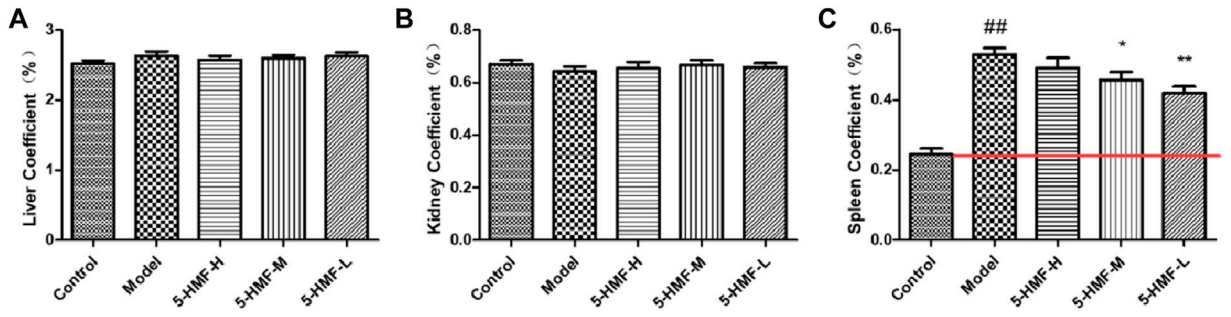

FIGURE 2 | Organ index of mice in the control group and model group treated with saline (model) and different doses of 5-HMF. **(A)** Liver index. **(B)** Kidney index. **(C)** Spleen index. Each value represents the mean SD (n = 8); $^{\#\#}p < 0.01$, compared with the control group; $^{*}p < 0.05$ and $^{**}p < 0.01$, compared with the model group.

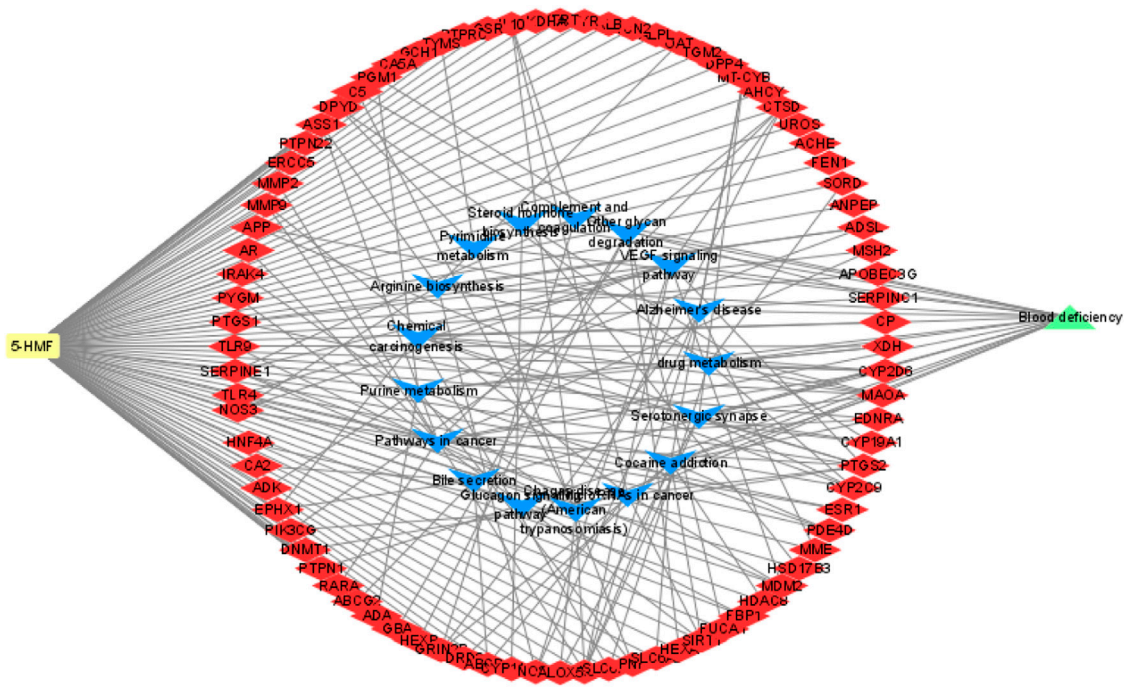

FIGURE 3 | The blue triangle node represents the common pathway of 5-HMF and BDS, while the red quadrilateral node represents the common target of 5-HMF and BDS.

A) and acetonitrile and 0.1% formic acid (phase B). The elution gradient of phase B was as follows: 2% (0–0.5 min), 2% up to 40% (0.5–9 min), 40% up to 98% (9–16 min), then maintained at 98% for 1 min. Optimized parameters for the mass spectrometer were as follows: ion spray voltage, 5 or −4 kV (for positive and negative mode, respectively); declustering potential, 60 V; curtain gas, 25 psi; nebulizer gas of 40 psi; interface heater temperature, 650 C; scan range (m/z), 50–1,200. The stability of the analysis was continuously monitored by analyzing QC samples at intervals of every 10 samples.

2.6.3 Multivariate Data Analysis

The advanced Progressive QI platform (Waters, United States) was used to obtain potential and critical annotations from the original centroid data file obtained by SYNAPT G2-Si. Metabolic data completed by principal component analysis and dimensionality reduction had the most significant impact on health and disease. The potential differences in metabolites were identified from the orthogonal partial least squares discriminant analysis (OPLS-DA). The components that significantly impacted the grouping were screened out through objective numerical values. The t-test value was lower than 0.05.

2.6.4 Biomarker Identification and Metabolic Pathway Analysis

LC-MS/MS data were imported into Ezinfo software (Waters Progressional QI) for principal component analysis and OPLS-DA data analysis. The variable projection importance value

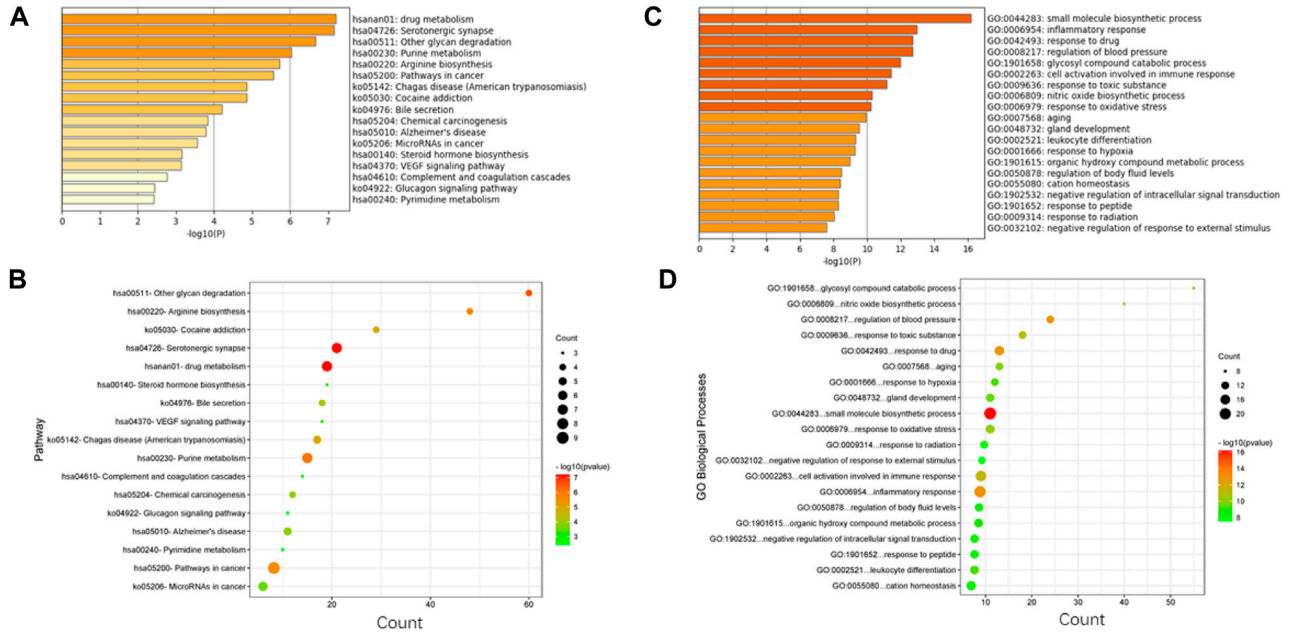

FIGURE 4 | (A) 5-HMF and BDS common target KEGG enrichment analysis; **(B)** 5-HMF and BDS common target KEGG enrichment analysis bubble chart; **(C)** 5-HMF and BDS common target GO enrichment analysis of dots; **(D)** Bubble chart of GO enrichment analysis of the common target of 5-HMF and BDS.

obtained by OPLS-DA was used to evaluate the impact of each metabolite difference on the discrimination and interpretation ability of each sample. The greater the VIP value, the more significant the contribution of metabolites to sample differentiation. It is generally believed that there are significant differences between variables with VIP >1. The potential biomarkers were the S-plot constructed by Ezinfo, and the V-plot was labeled.

2.7 Statistical Analysis

All data were expressed in terms of mean ± standard deviation. The two-tailed unpaired *t*-test was performed using SPSS 21.0 software (from SPSS Corporation, United States). A value of $p < 0.05$ was considered to show a significant difference. A value of $p < 0.01$ was considered to indicate a highly significant difference. The histogram was drawn by GraphPad Prism 7 software (GraphPad Software, United States).

2.7.1 Pathway Analysis

The targets from network pharmacology and the metabolites from plasma metabolomics were jointly analyzed by MetaboAnalyst to select crucial metabolism pathways.

2.8 Western Blot Was Applied to Verify the Expression of Common Key Proteins in Metabolomics and Network Pharmacology

The bincinchoninic acid (BCA) method was used to determine the total protein of conventionally extracted splenocytes. The extract was separated by 10% SDS polyacrylamide gel electrophoresis and transferred to the PVDF membrane. It was blocked with 5% skim milk at room temperature for 1 h, and antibodies of CYP17A1, HSD3B1 (all 1:1,000), and GAPDH (all 1:2,000) were added. These were incubated overnight at 4 C and rinsed with tris buffered saline with Tween 20 (TBST) three times for 10 min each. The membrane was immersed in the horseradish peroxidase-labeled secondary antibody (1:1,000), diluted in 2% skimmed milk, incubated at room temperature for 1 h, and rinsed with TBST 3 times, each for 10 min. Image Quant LAS 500 imaging equipment acquired the signal using the ECL chemiluminescence method.

3 RESULTS

3.1 Behavioral Analysis of Rats

Changes in the general behavior of rats could reflect the occurrence of and recovery from BDS in rats. After BDS induction, rats in the model group developed fatigue and lethargy, accompanied by weight loss, thinning hair, pale ears and tails, and loss of appetite. These symptoms were consistent with the description of BDS in Chinese medicine. In contrast, the control and BDS-induced rats treated with 5-HMF were relatively robust, showing thick and shiny hair, pink and moist nose and lips, round and pink tails, and stable body weight along with increased appetite.

3.2 Routine Blood Testing

After 15 days of administration of normal saline and 5-HMF, the RBC, WBC, HGB, and HCT levels in the peripheral blood of the rats were measured (**Figure 1**). Compared with the control group, the RBC, WBC, HGB, and HCT levels in the model group were significantly reduced ($p < 0.01$), indicating that the blood

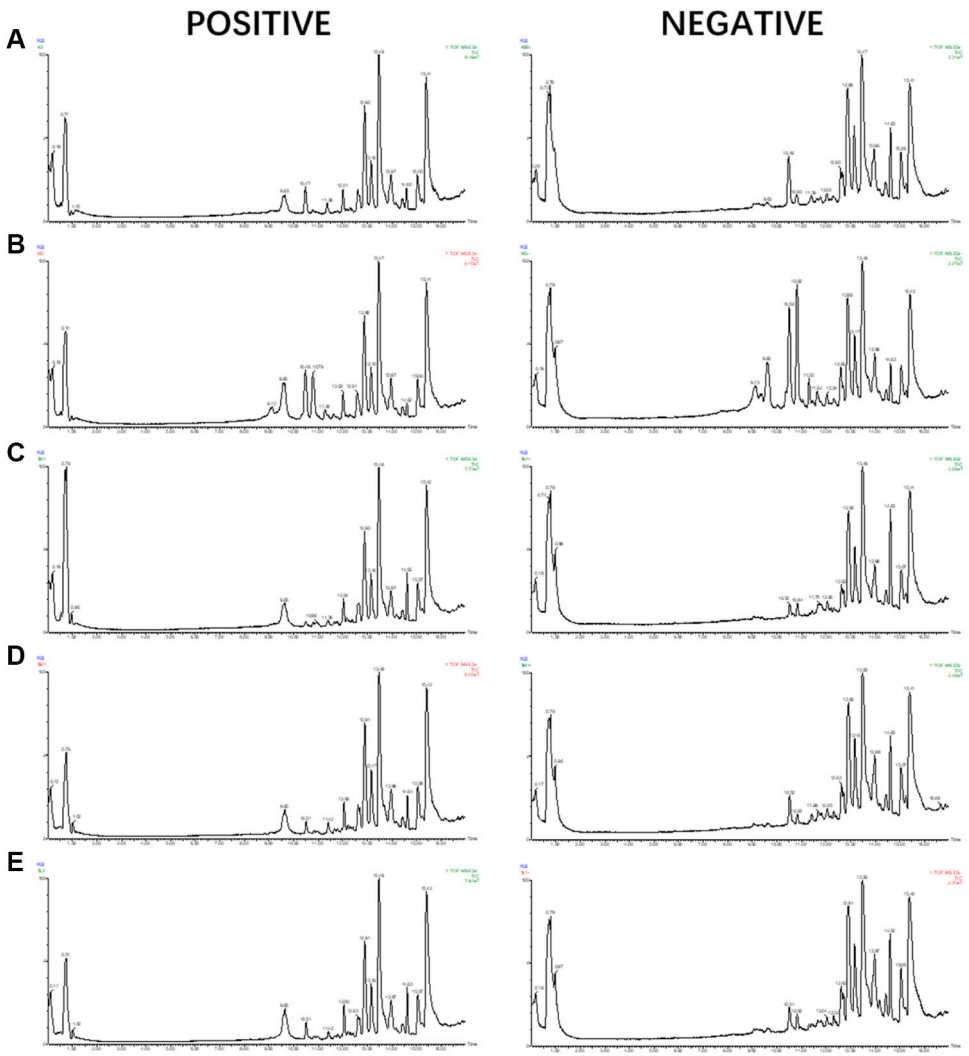

FIGURE 5 | UPLC-MS/MS TIC diagram: **(A)** Control group, **(B)** Model group **(C)** 5-HMF-H group, **(D)** 5-HMF-M group, **(E)** 5-HMF- L group.

deficiency model was successfully established. The levels of WBC, RBC, HGB, and HCT in the Model group were significantly increased after 5-HMF treatment ($p < 0.05$ or $p < 0.01$).

3.3 Organ Index

The results of the organ index are shown in **Figure 2** Compared with the control group, the liver and kidney function in the model group were relatively unchanged, but the spleen was abnormally enlarged. Except for the spleen coefficient, the experimental group (model group, 5-HMF-H group, 5-HMF-M group, and 5-HMF-L group) and the control group had no significant differences in other organ coefficients. Compared with the control group, the spleen coefficient in the model group increased significantly ($p < 0.01$). Compared with the model group, the spleen coefficient in the 5-HMF-L group was significantly reduced ($p < 0.01$), the spleen coefficient in the 5-HMF-M group was decreased significantly ($p < 0.05$), and the spleen coefficient in the 5-HMF-H group was not very different. The results showed that 5-HMF had a dose-dependent reversal effect on spleen enlargement.

3.4 Results of Network Pharmacology Analysis

3.4.1 5-Hydromethylfurfural and Blood Deficiency Syndrome Common Target Interaction

In this study, four online websites were used to predict 5-HMF targets, and three were used to predict BDS disease targets. Finally, it was determined that 5-HMF had 494 targets, BDS had a total of 1887 targets, and a total of 84 common targets. To further explore the mechanism of 5-HMF treatment of BDS, KEGG enrichment analysis was performed on 84 common targets, and 14 metabolic pathways were obtained (**Figure 3**), and the common targets and pathways are illustrated in a network diagram (**Figure 4**). The results show that the 5-HMF

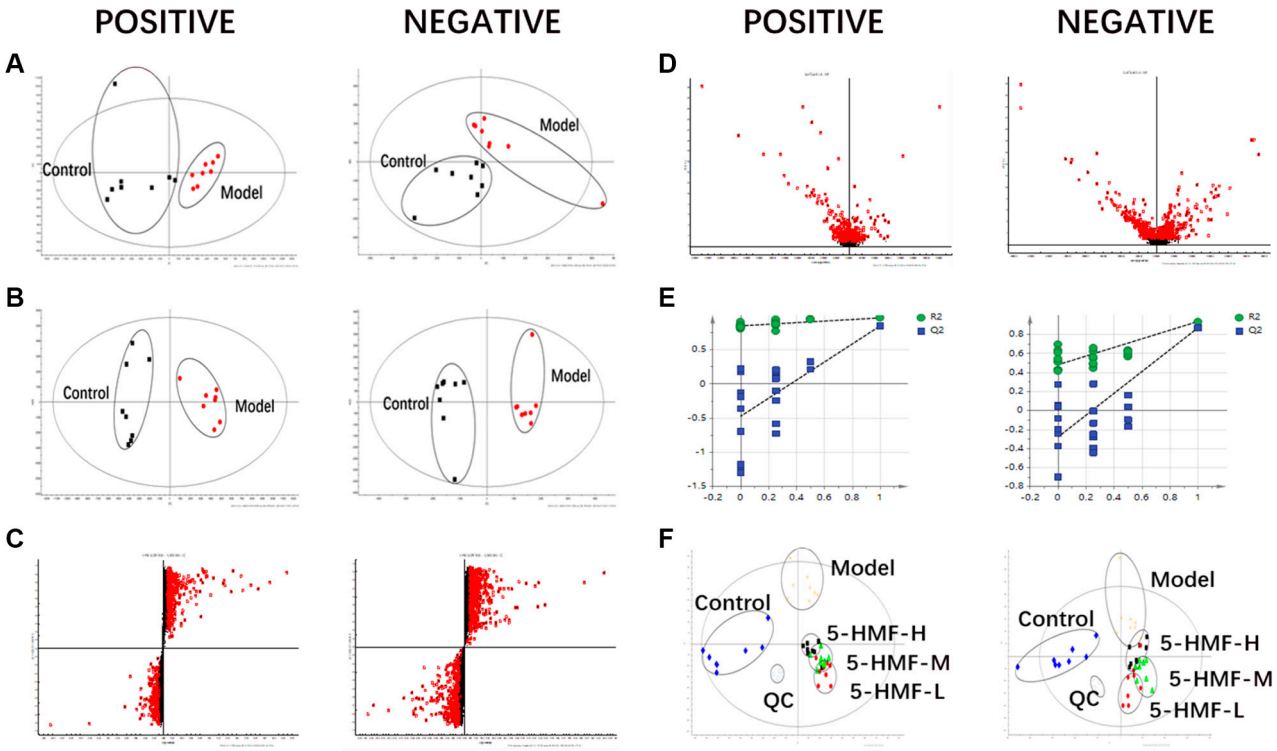

FIGURE 6 | Multivariate data of UPLC-MS/MS: **(A)** Principal Component Analysis Score Chart, **(B)** OPLS-DA Analysis Score Chart **(C)** OPLS-DA S-plot Chart, **(D)** OPLS-DA V-plot Chart **(E)** Partial Least Squares-Data Analysis Model Validation Diagram, **(F)** PLS-DA Analysis Score Diagram. Plasma samples were collected from the different groups.

treatment of BDS has the characteristics of multiple pathways and multiple targets.

3.5 Results of Metabolomics Analysis

3.5.1 Multivariate Data Analysis

The samples were analyzed with the UPLC/Q-TOF metabolic spectrum. No abnormalities were found in the total ion chromatogram, and the retention time of chromatographic peaks and their ionic strength were observed (**Figure 5**) Masslynx and Progenesis QI software were used to analyze many raw files from G2-Si total quantification for data preprocessing, such as peak picking, denoising, and normalization, to generate a bioinformatics matrix. Then we exported the data set to Simca 14.1 software for chemometric analysis. The principal component analysis score chart showed that the model group was separated from the control group (**Figure 6A**). A significant separation between the model group and the control group was observed in the OPLS-DA chart (**Figure 6B**). The S-plot of OPLS-DA showed multiple metabolites (**Figure 6C**). The V-plot diagram of OPLS-DA showed a remarkable diversity of various metabolites (**Figure 6D**). The replacement test was used to verify the OPLS-DA mode (**Figure 6E**). **Figure 6F** shows that all experimental groups were separate in the liquid chromatography-mass spectrometry metabolic map. Among them, the metabolic profiles of the 5-HMF-H group, 5-HMF-M group, and 5-HMF-L group were closer to the control group than the model group, suggesting that the model's metabolic disorder that was induced was reversed after drug treatment, and the 5-HMF-L group had a better separation effect. The four points in the QC group were in clustered, which proved that the machine was stable.

3.5.2 Identification of Endogenous Metabolites

The difference metabolites between the control group and the model group were screened according to the VIP value (VIP >1.0) and *t*-test ($p < 0.05$). As a result, a total of 65 different metabolites were screened (**Table 1**). Compared with the control group, 35 different metabolites (epitestosterone, etc.) were significantly increased, and 30 different metabolites (17a-hydroxypregnenolone, etc.) significantly reduced. The 5-HMF-H group could regulate 48 metabolites (p-xanthine, etc.). The 5-HMF-M group could regulate 50 kinds of metabolites (5-KETE, etc.). The 5-HMF-L group could regulate 57 metabolites (5-KETE, etc.). The 5-HMF-L group had significantly more metabolic differences than the other two groups.

There were 9 metabolites involved in metabolism in the control group, model group, and 5-HMF-L group (**Figure 7**). To further clarify the distribution of 9 different metabolites in different groups, unsupervised clustering was performed by using a hierarchical clustering analysis heat map. As shown in **Figure 8**, there were significant differences between the model group and

TABLE 1 | Detection of BDS-related Metabolites in Plasma by LC-MS. Trend 1 is Control group compared with Model group; Trend 2 is Model group compared with 5-HML-L group.

NO.	Metabolites	TR (min)	m/z	Formula	VIP	*p* Value	Fold change	Trend 1	Trend 2	HMDB ID	Scan mode
1	PC(20:5 (5Z,8Z,11Z,14Z,17Z)/P-16:0)	20.98	764.5597	$C_{44}H_{78}NO_7P$	1.34	4.60E-02	1.14	↑	—	8,521	+
2	PC(18:2 (9Z,12Z)/P-16:0)	20.91	764.5466	$C_{42}H_{80}NO_7P$	1.51	3.11E-02	1.10	—	↑	8,159	+
3	Trihexosylceramide (d18:1/12:0)	20.71	985.6484	$C_{48}H_{89}NO_{18}$	1.39	4.09E-02	1.21	—	↓	4,877	+
4	Trihexosylceramide (d18:1/16:0)	20.70	1,041.7068	$C_{52}H_{97}NO_{18}$	4.17	6.76E-05	1.57	—	↓	4,879	+
5	LysoPC(22:2 (13Z,16Z))	20.68	593.4293	$C_{30}H_{58}NO_7P$	7.26	5.55E-08	1.47	—	↓	10400	+
6	DG (16:0/20:0/0:0)	20.67	647.5559	$C_{39}H_{76}O_5$	1.90	1.26E-02	1.12	—	↓	7,107	+
7	DG (16:0/18:0/0:0)	20.65	596.9646	$C_{37}H_{72}O_5$	2.02	9.58E-03	1.31	↑	↓	7,100	+
8	CE (18:3 (9Z,12Z,15Z))	20.64	669.5554	$C_{45}H_{74}O_2$	7.65	2.23E-08	1.72	—	↓	10370	+
9	2,5-Furandicarboxylic acid	20.59	201.0376	$C_6H_4O_5$	6.53	2.93E-07	1.30	—	↑	4,812	-
10	Phytofluene	20.39	542.9203	$C_{40}H_{62}$	3.83	1.46E-04	3.22	↑	—	2871	+
11	Oleamide	20.27	282.2829	$C_{18}H_{35}NO$	2.39	4.10E-03	1.64	↑	—	2117	+
12	PC(20:0/18:4 (6Z,9Z,12Z,15Z))	20.18	810.1348	$C_{46}H_{84}NO_8P$	2.18	6.63E-03	1.60	↓	—	8,273	+
13	PC(20:4 (8Z,11Z,14Z,17Z)/18:0)	20.12	810.1348	$C_{46}H_{84}NO_8P$	3.93	1.16E-04	2.56	↓	—	8,464	+
14	PC(18:2 (9Z,12Z)/P-18:1 (11Z))	20.11	768.0981	$C_{44}H_{82}NO_7P$	1.80	1.58E-02	1.41	↓	—	8,161	+
15	PC(16:1 (9Z)/22:2 (13Z,16Z))	20.07	810.5913	$C_{46}H_{86}NO_8P$	2.95	1.12E-03	1.57	—	↓	8,020	-
16	PC(18:0/P-18:1 (11Z))	20.05	770.5976	$C_{44}H_{86}NO_7P$	2.91	1.22E-03	1.44	—	↑	8,062	-
17	PC(16:0/P-18:1 (11Z))	20.02	742.5653	$C_{42}H_{82}NO_7P$	2.05	8.90E-03	1.57	—	↓	7,996	-
18	LysoPC(22:1 (13Z))	19.95	577.7737	$C_{30}H_{60}NO_7P$	1.69	2.05E-02	1.14	↓	-	10399	+
19	PC(18:0/14:0)	19.94	734.5788	$C_{40}H_{80}NO_8P$	4.23	5.88E-05	1.48	—	↓	8,031	+
20	Arachidonic acid	19.94	304.4669	$C_{20}H_{32}O_2$	2.93	1.18E-03	1.99	↑	—	1,043	-
21	PI(18:2 (9Z,12Z)/16:0)	19.94	852.5681	$C_{43}H_{79}O_{13}P$	2.95	1.11E-03	1.22	—	↓	9846	+
22	PC(20:1 (11Z)/P-16:0)	19.94	794.6085	$C_{44}H_{86}NO_7P$	8.07	8.47E-09	1.44	—	↑	8,324	+
23	PC(18:3 (9Z,12Z,15Z)/P-18:0)	19.94	768.5950	$C_{44}H_{82}NO_7P$	2.40	3.98E-03	1.40	—	↑	8,226	+
24	PC(20:4 (8Z,11Z,14Z,17Z)/16:0)	19.93	782.0817	$C_{44}H_{80}NO_8P$	9.10	7.91E-10	7.06	↑	—	8,462	+
25	PI(22:4 (7Z,10Z,13Z,16Z)/16:0)	19.93	887.5759	$C_{47}H_{83}O_{13}P$	3.77	1.70E-04	1.13	—	↓	9914	+
26	PC(20:2 (11Z,14Z)/14:0)	18.77	758.0603	$C_{42}H_{80}NO_8P$	1.85	1.40E-02	2.92	↑	—	8,328	+
27	PC(18:2 (9Z,12Z)/18:1 (9Z))	18.71	784.5924	$C_{44}H_{82}NO_8P$	2.63	2.34E-03	1.26	—	↓	8,137	+
28	PI(16:0/20:0)	18.71	911.5975	$C_{45}H_{87}O_{13}P$	4.67	2.16E-05	3.18	—	↑	9785	—
29	PC(18:4 (6Z,9Z,12Z,15Z)/18:1 (9Z))	18.71	780.0658	$C_{44}H_{78}NO_8P$	7.19	6.53E-08	6.71	↑	—	8,236	+
30	Trihexosylceramide (d18:1/24:0)	18.71	1,158.7722	$C_{60}H_{113}NO_{18}$	4.80	1.58E-05	1.26	—	↓	4,886	+
31	DG (16:1 (9Z)/18:2 (9Z,12Z)/0:0)	18.70	591.5034	$C_{37}H_{66}O_5$	15.11	7.77E-16	3.03	—	↓	7,132	+

(Continued on following page)

TABLE 1 | (*Continued*) Detection of BDS-related Metabolites in Plasma by LC-MS. Trend 1 is Control group compared with Model group; Trend 2 is Model group compared with 5-HML-L group.

NO.	Metabolites	TR (min)	m/z	Formula	VIP	*p* Value	Fold change	Trend 1	Trend 2	HMDB ID	Scan mode
32	DG (16:0/16:0/0:0)	18.69	568.9114	$C_{35}H_{68}O_5$	1.60	2.50E-02	1.15	↑	↓	7,098	+
33	CE (22:5 (7Z,10Z,13Z,16Z,19Z))	18.69	721.5887	$C_{49}H_{78}O_2$	12.48	3.31E-13	2.25	—	↓	10375	+
34	D-Erythrose 4-phosphate	18.69	245.0038	$C_4H_9O_7P$	5.49	3.20E-06	1.28	—	↑	1,321	-
35	LysoPC(22:6 (4Z,7Z,10Z,13Z,16Z,19Z))	18.67	567.6943	$C_{30}H_{50}NO_7P$	3.99	1.02E-04	4.47	↓	-	10404	+
36	Glucosylceramide (d18:1/12:0)	18.63	644.5063	$C_{36}H_{69}NO_8$	5.40	3.99E-06	1.25	—	↓	4,969	+
37	S-Adenosylmethionine	17.87	399.4450	$C_{15}H_{23}N_6O_5S+$	1.99	1.03E-02	1.86	↑	—	1,185	—
38	SM(d18:0/14:1 (9Z) (OH))	17.84	689.5316	$C_{37}H_{73}N_2O_7P$	2.41	3.92E-03	1.39	—	↓	13462	+
39	PC(16:1 (9Z)/P-16:0)	17.83	733.5758	$C_{40}H_{78}NO_7P$	5.36	4.39E-06	1.45	-	↓	8,027	+
40	PC(20:3 (5Z,8Z,11Z)/P-18:1 (11Z))	17.82	816.6024	$C_{46}H_{84}NO_7P$	5.09	8.06E-06	1.43	—	↑	8,392	+
41	DG (18:1 (9Z)/18:2 (9Z,12Z)/0:0)	17.82	618.9701	$C_{39}H_{70}O_5$	2.48	3.33E-03	1.26	↑	—	7,219	+
42	Secoisolariciresinol	17.81	407.1669	$C_{20}H_{26}O_6$	3.11	7.70E-04	1.32	—	↓	13692	—
43	PC(22:2 (13Z,16Z)/14:0)	17.81	786.1134	$C_{44}H_{84}NO_8P$	2.20	6.34E-03	1.26	↓	—	8,590	+
44	17a-Hydroxypregnenolone	17.79	332.4770	$C_{21}H_{32}O_3$	2.92	1.20E-03	1.61	↓	↑	363	+
45	PI(22:5 (7Z,10Z,13Z,16Z,19Z)/18:0)	17.68	913.1652	$C_{49}H_{85}O_{13}P$	2.91	1.23E-03	2.77	↑	—	9919	—
46	DG (18:1 (9Z)/20:0/0:0)	17.61	668.6202	$C_{41}H_{78}O_5$	6.38	4.20E-07	2.13	—	↓	7,223	+
47	PC(18:0/20:3 (8Z,11Z,14Z))	17.59	812.6229	$C_{46}H_{86}NO_8P$	2.33	4.69E-03	1.41	—	↓	8,047	+
48	SM(d18:0/16:1 (9Z) (OH))	17.59	717.5618	$C_{39}H_{77}N_2O_7P$	1.98	1.05E-02	1.38	—	↓	13463	+
49	SM(d18:0/16:1 (9Z))	17.59	703.5811	$C_{39}H_{79}N_2O_6P$	1.40	3.97E-02	1.14	—	↓	13464	+
50	PC(20:3 (8Z,11Z,14Z)/14:0)	17.58	756.0444	$C_{42}H_{78}NO_8P$	1.51	3.10E-02	1.39	↑	—	8,394	+
51	LysoPC(22:0)	17.57	579.7895	$C_{30}H_{62}NO_7P$	2.26	5.51E-03	1.34	↓	—	10398	+
52	PI(16:0/18:0)	17.32	856.5954	$C_{43}H_{83}O_{13}P$	5.57	2.71E-06	1.54	—	↑	9781	+
53	PC(22:5 (7Z,10Z,13Z,16Z,19Z)/16:0)	17.31	808.1189	$C_{46}H_{82}NO_8P$	5.60	2.53E-06	3.07	↑	↓	8,692	+
54	Ceramide (d18:1/25:0)	17.29	664.1399	$C_{43}H_{85}NO_3$	3.97	1.06E-04	11.72	↓	—	4,957	+
55	Glucosylceramide (d18:1/9Z-18:1)	17.19	726.0786	$C_{42}H_{79}NO_8$	3.56	2.76E-04	1.47	↑	—	4,970	—
56	beta-Cryptoxanthin	16.94	552.8870	$C_{40}H_{56}O$	3.43	3.69E-04	1.90	↓	—	33844	+
57	9,10-Epoxyoctadecenoic acid	16.50	296.4449	$C_{18}H_{32}O_3$	3.04	9.10E-04	1.27	↑	—	4,701	+
58	Adrenoyl ethanolamide	16.47	375.5878	$C_{24}H_{41}NO_2$	2.10	7.90E-03	1.72	↑	—	13626	+
59	LysoPC(22:5 (4Z,7Z,10Z,13Z,16Z))	16.41	569.7101	$C_{30}H_{52}NO_7P$	3.22	6.07E-04	1.56	↓	—	10402	+
60	Chenodeoxycholic acid	15.90	393.3044	$C_{24}H_{40}O_4$	2.20	6.35E-03	1.09	—	↑	518	+
61	Cer(d18:1/14:0)	15.43	508.4804	$C_{32}H_{63}NO_3$	1.55	2.85E-02	1.48	—	↓	11773	—
62	LysoPC(20:3 (5Z,8Z,11Z))	15.42	546.3631	$C_{28}H_{52}NO_7P$	2.05	8.89E-03	1.11	—	↑	10393	+

(Continued on following page)

TABLE 1 | (*Continued*) Detection of BDS-related Metabolites in Plasma by LC-MS. Trend 1 is Control group compared with Model group; Trend 2 is Model group compared with 5-HML-L group.

NO.	Metabolites	TR (min)	m/z	Formula	VIP	*p* Value	Fold change	Trend 1	Trend 2	HMDB ID	Scan mode
63	PC(24:1 (15Z)/P-18:1 (11Z))	15.40	898.6832	$C_{50}H_{96}NO_7P$	1.52	2.99E-02	6.92	—	↓	8,819	—
64	PC(22:2 (13Z,16Z)/P-18:1 (11Z))	15.36	868.6364	$C_{48}H_{90}NO_7P$	1.59	2.58E-02	2.14	—	↓	8,621	—
65	Docosahexaenoic acid	14.85	328.4883	$C_{22}H_{32}O_2$	3.07	8.49E-04	2.13	↑	—	2183	+
66	PC(14:0/18:3 (6Z,9Z,12Z))	14.63	745.5483	$C_{40}H_{74}NO_8P$	8.01	9.74E-09	2.41	—	↓	7,875	+
67	Retinal	14.62	284.4357	$C_{20}H_{28}O$	1.42	3.83E-02	1.72	↑	—	1,358	+
68	Dihydrofolic acid	14.51	443.4133	$C_{19}H_{21}N_7O_6$	1.52	3.03E-02	2.22	↑	—	1,056	—
69	PC(20:5 (5Z,8Z,11Z,14Z,17Z)/P-18:1 (11Z))	14.46	834.5671	$C_{46}H_{80}NO_7P$	4.13	7.48E-05	3.39	—	↑	8,523	—
70	N1,N12-Diacetylspermine	14.28	286.4136	$C_{14}H_{30}N_4O_2$	2.42	3.82E-03	3.41	↑	—	2172	—
71	LysoPC(22:4 (7Z,10Z,13Z,16Z))	14.25	571.7260	$C_{30}H_{54}NO_7P$	3.14	7.20E-04	1.41	↓	↑	10401	—
72	LysoPC(20:2 (11Z,14Z))	14.20	547.7046	$C_{28}H_{54}NO_7P$	2.72	1.89E-03	1.19	↓	—	10392	—
73	PC(20:4 (8Z,11Z,14Z,17Z)/P-18:1 (9Z))	14.06	792.1195	$C_{46}H_{82}NO_7P$	3.61	2.47E-04	2.05	↑	—	8,491	—
74	PC(22:6 (4Z,7Z,10Z,13Z,16Z,19Z)/P-18:0)	14.05	818.1568	$C_{48}H_{84}NO_7P$	4.43	3.73E-05	2.42	↑	—	8,752	—
75	PC(22:4 (7Z,10Z,13Z,16Z)/P-16:0)	13.98	794.1354	$C_{46}H_{84}NO_7P$	2.53	2.98E-03	3.69	↑	—	8,652	—
76	all-trans-Retinoic acid	13.73	300.4420	$C_{20}H_{28}O_2$	2.86	1.37E-03	3.46	↑	—	1852	+
77	PC(18:4 (6Z,9Z,12Z,15Z)/P-18:1 (11Z))	13.62	808.5438	$C_{44}H_{78}NO_7P$	2.18	6.63E-03	2.28	—	↑	8,260	—
78	PS(18:0/18:1 (9Z))	13.60	788.5432	$C_{42}H_{80}NO_{10}P$	2.71	1.93E-03	1.32	—	↓	10163	—
79	Ceramide (d18:1/12:0)	13.53	480.4446	$C_{30}H_{59}NO_3$	1.76	1.75E-02	1.24	—	↓	4,947	—
80	Ubiquinone-1	13.43	250.2903	$C_{14}H_{18}O_4$	1.82	1.52E-02	1.41	↓	↑	2012	+
81	L-Cystathionine	13.16	222.2620	$C_7H_{14}N_2O_4S$	3.21	6.19E-04	1.30	↓	↑	99	+
82	L-Palmitoylcarnitine	12.95	400.6230	$C_{23}H_{45}NO_4$	4.43	3.70E-05	1.76	↑	—	222	+
83	Ganglioside GM3 (d18:1/16:0)	12.93	1,151.6951	$C_{57}H_{104}N_2O_{21}$	5.30	4.99E-06	1.24	—	↑	4,844	—
84	PS(18:0/22:6 (4Z,7Z,10Z,13Z,16Z,19Z))	12.69	836.0860	$C_{46}H_{78}NO_{10}P$	5.28	5.30E-06	6.79	↓	—	10167	—
85	LysoPC(18:2 (9Z,12Z))	12.67	519.6515	$C_{26}H_{50}NO_7P$	3.97	1.06E-04	1.26	↓	—	10386	—
86	5-KETE	12.41	318.4504	$C_{20}H_{30}O_3$	5.22	6.06E-06	8.58	↓	—	10217	—
87	PS(18:0/20:4 (8Z,11Z,14Z,17Z))	12.40	812.0646	$C_{44}H_{78}NO_{10}P$	3.45	3.54E-04	9.39	↓	—	10165	—
88	PC(18:3 (6Z,9Z,12Z)/P-18:1 (11Z))	12.40	810.5626	$C_{44}H_{80}NO_7P$	3.30	4.96E-04	6.75	—	↑	8,194	—
89	13-cis-Retinoic acid	12.33	300.4351	$C_{20}H_{28}O_2$	4.53	2.93E-05	7.08	↓	—	6219	+
90	LysoPC(16:1 (9Z)/0:0)	12.30	493.6142	$C_{24}H_{48}NO_7P$	1.93	1.17E-02	1.45	↑	—	10383	+
91	2-Methoxyestrone	12.06	300.3921	$C_{19}H_{24}O_3$	5.28	5.29E-06	5.28	↓	—	10	—
92	LysoPC(14:0/0:0)	11.80	467.5769	$C_{22}H_{46}NO_7P$	1.56	2.73E-02	1.37	↑	—	10379	+
93	Testosterone glucuronide	11.74	464.5485	$C_{25}H_{36}O_8$	3.81	1.56E-04	2.12	↑	—	3,193	-

(Continued on following page)

TABLE 1 | (*Continued*) Detection of BDS-related Metabolites in Plasma by LC-MS. Trend 1 is Control group compared with Model group; Trend 2 is Model group compared with 5-HML-L group.

NO.	Metabolites	TR (min)	m/z	Formula	VIP	*p* Value	Fold change	Trend 1	Trend 2	HMDB ID	Scan mode
94	Sphinganine	11.67	301.5078	$C_{18}H_{39}NO_2$	2.85	1.43E-03	1.58	↑	—	269	+
95	Sphingosine 1-phosphate	11.65	379.4718	$C_{18}H_{38}NO_5P$	4.85	1.42E-05	2.46	↑	—	277	+
96	15-Deoxy-d-12,14-PGJ2	11.51	316.4345	$C_{20}H_{28}O_3$	5.39	4.09E-06	5.56	↓	↑	5079	—
97	Delta-12-Prostaglandin J2	11.34	334.4498	$C_{20}H_{30}O_4$	2.79	1.64E-03	2.15	↓	—	4,238	—
98	Dehydroepiandrosterone	11.15	288.4244	$C_{19}H_{28}O_2$	2.75	1.76E-03	2.16	↓	—	77	—
99	(9xi,10xi,12xi)-9,10-Dihydroxy-12-octadecenoic acid	10.93	314.4660	$C_{18}H_{34}O_4$	3.56	2.75E-04	22.15	↑	—	31679	—
100	LysoPC(20:5 (5Z,8Z,11Z,14Z,17Z))	10.64	541.6570	$C_{28}H_{48}NO_7P$	1.73	1.88E-02	1.65	↑	—	10397	+
101	15(S)-HPETE	10.49	336.4657	$C_{20}H_{32}O_4$	3.91	1.22E-04	4.49	↓	—	4,244	—
102	Estrone	10.26	270.3661	$C_{18}H_{22}O_2$	4.97	1.08E-05	4.93	↓	—	145	—
103	11,12,15-THETA	10.18	354.4810	$C_{20}H_{34}O_5$	4.67	2.15E-05	3.48	↑	—	4,684	—
104	Palmitic acid	9.55	256.4241	$C_{16}H_{32}O_2$	2.83	1.47E-03	1.29	↑	—	220	+
105	11b-Hydroxyprogesterone	9.46	330.4611	$C_{20}H_{28}O_4$	4.70	2.00E-05	6.23	↓	—	4,031	—
106	Androstenedione	9.31	286.4085	$C_{19}H_{26}O_2$	1.73	1.87E-02	5.19	↓	—	53	—
107	Allopregnanolone	9.16	363.2590	$C_{21}H_{34}O_2$	1.42	3.77E-02	7.00	—	↓	1,449	—
108	Pyridoxamine 5′-phosphate	0.80	249.0656	$C_8H_{13}N_2O_5P$	1.87	1.33E-02	1.17	—	↑	1,555	+
109	Paraxanthine	0.78	180.1640	$C_7H_8N_4O_2$	2.96	1.09E-03	1.53	↓	↑	1860	+
110	Indoleacetic acid	0.75	176.0683	$C_{10}H_9NO_2$	2.14	7.17E-03	1.14	—	↑	197	+
111	Pyridoxamine	0.70	168.1931	$C_8H_{12}N_2O_2$	2.17	6.73E-03	1.52	↓	—	1,431	—
112	15-KETE	0.17	341.2050	$C_{20}H_{30}O_3$	2.81	1.55E-03	1.51	—	↑	10210	+
113	DG (18:2 (9Z,12Z)/20:1 (11Z)/0:0)	0.05	647.5553	$C_{41}H_{74}O_5$	1.41	3.87E-02	1.54	—	↓	7,253	+

the control group. These metabolites could be significantly regulated, and metabolic disorders in rats after 5-HMF treatment were improved.

3.5.3 Analysis of Metabolic Pathways

The metabolites of the 5-HMF-L group were input into MetaboAnalyst to explore the metabolic pathways of 5-HMF in the treatment of BDS. The results showed that the 5-HMF-L group may play a role through metabolism of cysteine, methionine, glycerophospholipid, sphingolipid, caffeine, vitamin B6, glycerol, and tyrosine and steroid hormone biosynthesis (**Figure 9**).

3.5.4 Pathway Analysis of Targets and Metabolites

To explore the crucial metabolic pathways, joint pathway analysis by MetaboAnalyst was conducted with the 57 differential metabolites and 84 targets. The results showed that only steroid hormone biosynthesis was simultaneously enriched with the targets from network pharmacology and the differential metabolites from metabolomics. According to the number of targets from the network pharmacology in the pathway, steroid hormones biosynthesis was selected as the most crucial metabolic pathway (**Figure 10**).

3.6 Effects of 5-Hydromethylfurfural on the Expression of Key Proteins in the Spleen of Blood Deficiency Rats

Compared with the control group, the expression of CYP17A1 and HSD3B1 protein in the spleen of the model group was decreased ($p < 0.05$). Compared with the model group, the 5-HMF-H group had increased expression of CYP17A1 protein ($p < 0.05$), and the 5-HMF-M and 5-HMF-L groups had significantly increased expression of CYP17A1 protein ($p <$

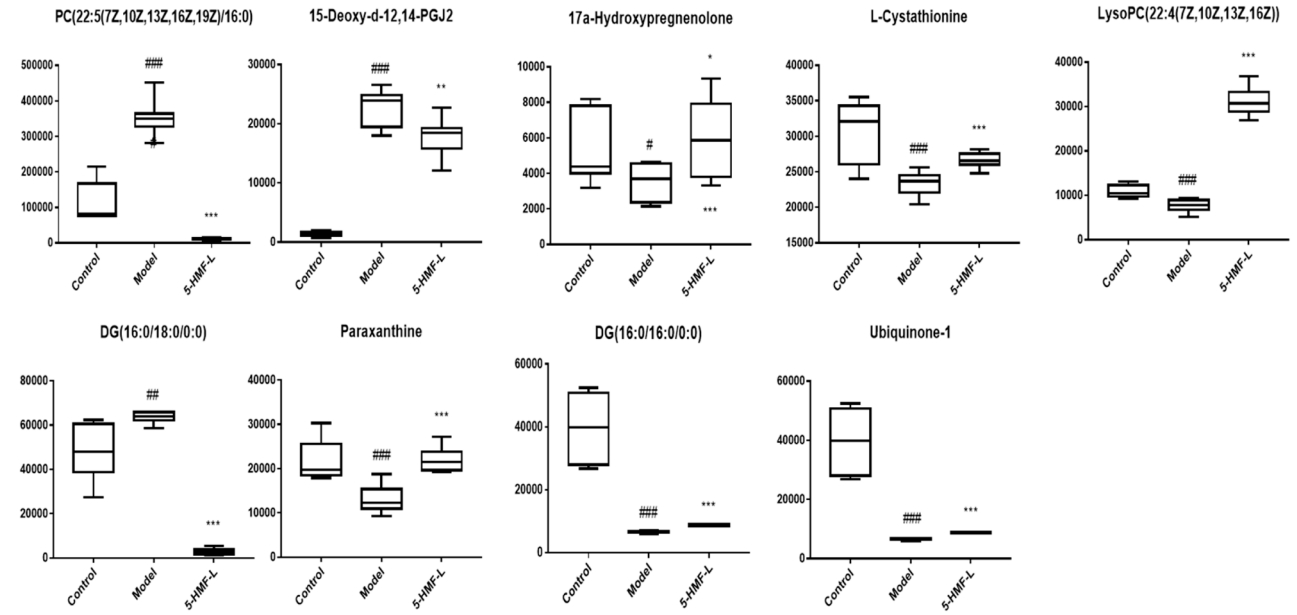

FIGURE 7 | Comparison of the relative content of different metabolites in plasma of the different administration groups. All data are expressed as mean ± standard deviation (n = 8). $^{\#}p < 0.05$, $^{\#\#}p < 0.01$, $^{\#\#\#}p < 0.001$ compared with the control group; $^{*}p < 0.05$, $^{***}p < 0.001$ compared with the model group.

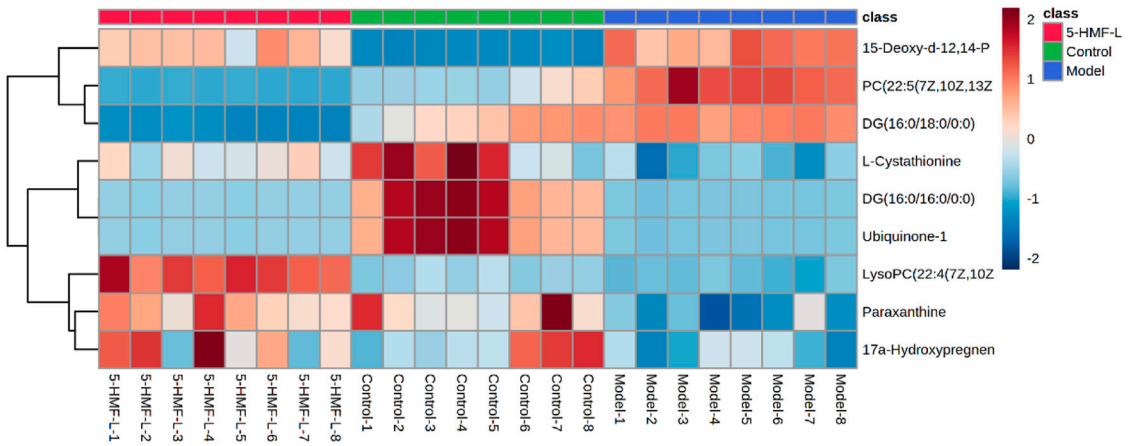

FIGURE 8 | Cluster analysis heatmap of different metabolites in BDS rat plasma. Brown and blue represent higher and lower than average levels of different metabolites, respectively. The rows represent different metabolites, and the columns represent rat plasma samples (n = 8).

0.01). Compared with the model group, the 5-HMF-L group had increased expression of HSD3B1 protein ($p < 0.05$) (**Figure 11**).

4 DISCUSSION

According to the theory of TCM, the pathogenesis of BDS might be qi-blood discord, the imbalance between yin and yang, blood stasis, and visceral dysfunction. Therefore, Chinese herbal medicines that could nourish yin and blood, fill the essence, and nourish the marrow were often used clinically to treat BDS and anemia (Bailly et al., 1978). Another medicine, RP, has been used for more than 1,000 years to nourish yin and blood, but the possible mechanism of the effect of "tonifying blood" is still unclear. The appearance of rats in the model group changed significantly, including hair loss, slow movement, and weight loss. From the behavior of BDS rats, 5-HMF was effective in treating BDS. Peripheral RBC, WBC, HGB, and HCT were significantly reduced, a typical clinical manifestation of BDS and anemia (Safeukui et al., 2015). At the same time, the 5-HMF-H group did not have increases in WBC, RBC, and HGB, but the 5-HMF-M group and the 5-HMF-L group had more obvious therapeutic effects. Another indication of anemia is splenomegaly, which is one of the most common and earliest pathological manifestations

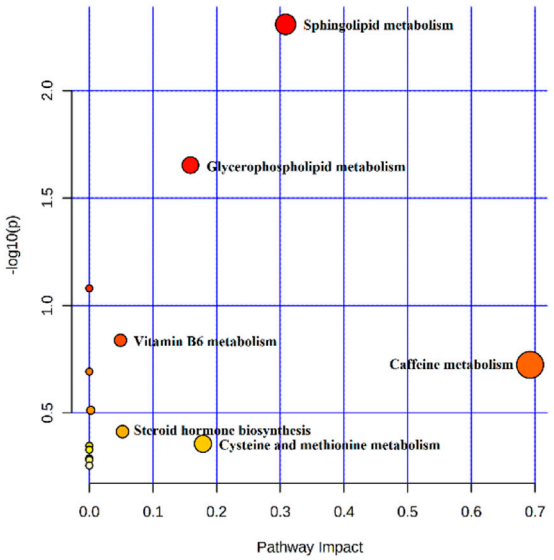

FIGURE 9 | Pathway analysis of plasma samples from BDS rats.

in different types of anemia (Altamura et al., 2019). It was generally believed that hematopoietic dysfunction was related to the discharge of bone marrow cells from bone marrow through blood, resulting in accumulation in the spleen (Koldkjaer et al., 2013). The collection of RBCs in the enlarged spleen could exacerbate anemia. Therefore, the reduction of RBCs in circulation and anemia are related to the degree of spleen enlargement (Gilep et al., 2011). According to **Figure 2**, the spleen mass in the model group was significantly greater than that in the control group. At the same time, compared with the model group, the spleen of the rats treated with 5-HMF was not enlarged. This showed that 5-HMF could reduce the side effects of chemotherapy on the spleen.

First, using the network pharmacology method, the therapeutic effect of 5-HMF on BDS was analyzed from the two perspectives of target and pathway. From the results of network pharmacology, the regulation of metabolic pathways might be one of the main mechanisms in 5-HMF treatment of BDS. Second, from the perspective of metabolomics, 5-HMF did have a curative effect on BDS, and the curative effect in the 5-HMF-L group was greater than that in the other two groups. Therefore, it showed the efficacy of 5-HMF in BDS treatment, and the most effective dose was in the 5-HMF-L group. Combined with network pharmacology and metabolomics analysis, the steroid hormone biosynthesis may be the key pathway of 5-HMF in the treatment of BDS.

Steroids are commonly used drugs to treat autoimmune hemolytic anemia, but long-term use of steroids can lead to drug resistance (Schiffer et al., 2019). Steroid hormones play a vital role in regulating water and salt balance, metabolism and stress response, and initiating and maintaining sexual differentiation and reproduction (Porcu et al., 2016). The production of new steroids produces steroid hormones in the adrenal cortex, gonads, and placenta. In addition, a series of neurosteroids are produced in the brain (Christakoudi et al., 2018; Sackett et al., 2018). They can promote the body's hematopoietic function, increase HGB, accelerate the circulation of oxygen and CO_2, and enhance physical strength (Wu et al., 2016).

The metabolic pathway of steroid hormone biosynthesis was entered into the KEGG database and compared with the

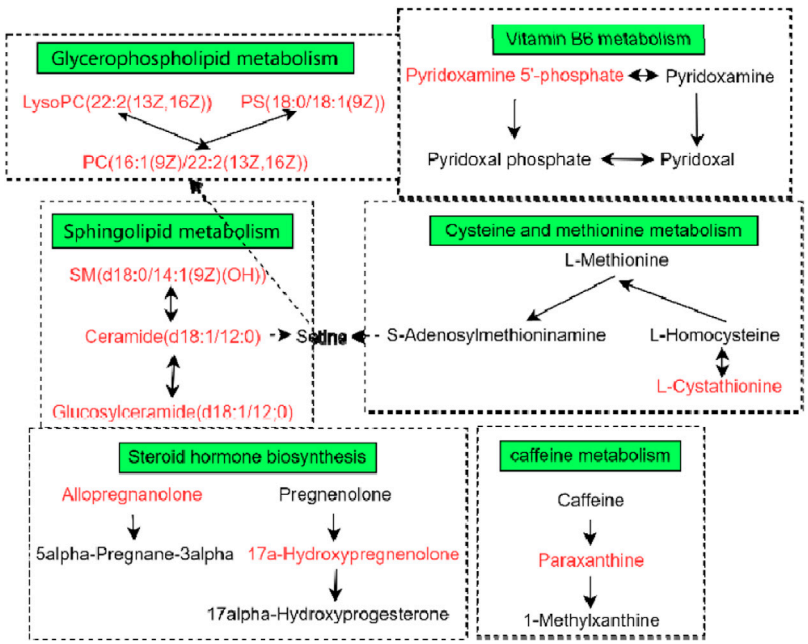

FIGURE 10 | Pathway analysis of plasma samples in 5-HMF-L group.

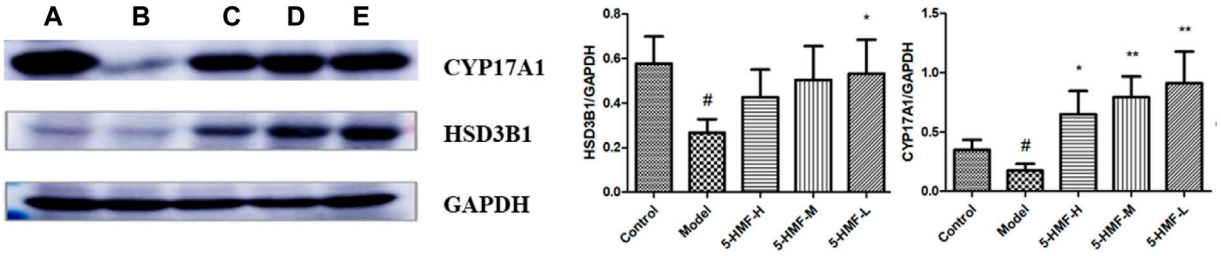

FIGURE 11 | Effect of each group on protein expression. **(A)** Control group, **(B)** Model group, **(C)** 5-HMF-H group, **(D)** 5-HMF-M group, **(E)** 5-HMF-L group. $^{\#}p < 0.05$, compared with the control group; $^{*}p < 0.05$ and $^{**}p < 0.01$, compared with the model group.

critical metabolic pathway genes predicted by network pharmacology. We found that CYP17A1 and HSD3B1 are essential proteins for steroid synthesis (Almassi et al., 2018). Western blot verified that in the 5-HMF-L group, the expression of CYP17A1 and HSD3B1 proteins was significantly up-regulated, which was consistent with the changing trends of metabolic results, verifying v the reliability of the metabolomics and network pharmacology prediction. Therefore, we have reason to believe that the steroid hormone biosynthesis pathway may be related to BDS and may be the potential mechanism of 5-HMF in the treatment of BDS. Our results suggest that 5-HMF provides a new therapeutic target by regulating related signaling pathways.

5 CONCLUSION

Our data showed that 5-HMF could ameliorate blood deficiency in rats induced by chemotherapy. Its mechanism might be regulating the expression of CYP17A1 and HSD3B1 in the steroid hormone biosynthesis pathway. These findings suggest that 5-HMF may be an effective alternative drug for BDS treatment.

DATA AVAILABILITY STATEMENT

The raw data supporting the conclusions of this article will be made available by the authors, without undue reservation.

ETHICS STATEMENT

The animal study was reviewed and approved by Ethics Committee of Heilongjiang University of Traditional Chinese Medicine.

AUTHOR CONTRIBUTIONS

WZ and NC have contributed equally to this work. HK and QW are responsible for this article.

FUNDING

Chief Scientist of Qi-Huang Project of National Traditional Chinese Medicine Inheritance and Innovation "One Hundred Million" Talent Project (2021). Qi-Huang Scholar of National Traditional Chinese Medicine Leading Talents Support Program (2018). Heilongjiang Touyan Innovation Team Program.

ACKNOWLEDGMENTS

The authors thank Charlesworth Author Services (www.dashboard.cwauthors.com.cn) for English language editing and review services.

REFERENCES

Almassi, N., Reichard, C., Li, J., Russell, C., Perry, J., Ryan, C. J., et al. (2018). HSD3B1 and Response to a Nonsteroidal CYP17A1 Inhibitor in Castration-Resistant Prostate Cancer. *JAMA Oncol.* 4 (4), 554–557. doi:10.1001/jamaoncol.2017.3159

Altamura, S., Vegi, N. M., Hoppe, P. S., Schroeder, T., Aichler, M., Walch, A., et al. (2019). Glutathione Peroxidase 4 and Vitamin E Control Reticulocyte Maturation, Stress Erythropoiesis and Iron Homeostasis. *Haematologica* 105 (4), 937–950. doi:10.3324/haematol.2018.212977

Amberger, J. S., Bocchini, C. A., Schiettecatte, F., Scott, A. F., and Hamosh, A. (2015). OMIM.org: Online Mendelian Inheritance in Man (OMIM®), an Online Catalog of Human Genes and Genetic Disorders. *Nucleic Acids Res.* 43 (Database issue), D789–D798. doi:10.1093/nar/gku1205

Bailly, Y., Sergant, M., and Raynaud, G. (1978). Hepato- and Thyreotoxicity of Tifemoxone. *Arch. Toxicol. Suppl.* 1, 229–233. doi:10.1007/978-3-642-66896-8_42

Brown, G. (2020). Towards a New Understanding of Decision-Making by Hematopoietic Stem Cells. *Int. J. Mol. Sci.* 21 (7), 2362. doi:10.3390/ijms21072362

Christakoudi, S., Runglall, M., Mobillo, P., Rebollo-Mesa, I., Tsui, T. L., Nova-Lamperti, E., et al. (2018). Steroid Regulation: An Overlooked Aspect of Tolerance and Chronic Rejection in Kidney Transplantation. *Mol. Cel Endocrinol* 473, 205–216. doi:10.1016/j.mce.2018.01.021

Duan, S. (2021). Effects of Angelica on Na~+-K~+-ATPase and Ca~(2+)-Mg~(2+)-ATPase in Blood Deficiency Rats[J]. *Gansu Anim. Husbandry Vet. Med.* 51 (04), 50–53.

Gfeller, D., Grosdidier, A., Wirth, M., Daina, A., Michielin, O., and Zoete, V. (2014). SwissTargetPrediction: a Web Server for Target Prediction of Bioactive Small Molecules. *Nucleic Acids Res.* 42 (Web Server issue), W32–W38. doi:10.1093/nar/gku293

Gilep, A. A., Sushko, T. A., and Usanov, S. A. (2011). At the Crossroads of Steroid Hormone Biosynthesis: the Role, Substrate Specificity and Evolutionary Development of CYP17. *Biochim. Biophys. Acta* 1814 (1), 200–209. doi:10.1016/j.bbapap.2010.06.021

Gong, W., Zhu, S., Chen, C., Yin, Q., Li, X., Du, G., et al. (2019). The Anti-depression Effect of Angelicae Sinensis Radix Is Related to the Pharmacological Activity of Modulating the Hematological Anomalies. *Front. Pharmacol.* 10, 192. doi:10.3389/fphar.2019.00192

Guo, Z. J., Zhai, H. Q., Yuan, Y. P., Zhang, T., Li, R., Kong, L. T., et al. (2016). National Physician Master Jin Shiyuan's Dispensing Technology of Rehmanniae Radix Praeparata Based on Li Shizhen's Pharmaceutical Academic Thought. *Zhongguo Zhong Yao Za Zhi* 41 (9), 1759–1762. Chinese. doi:10.4268/cjcmm20160930

Jiang, C., Lin, S. Y., and Zhao, J. L. (2013). Zhongguo Zhong Xi Yi Jie He Za Zhi Zhongguo Zhongxiyi Jiehe Zazhi = Chinese Journal of Integrated Traditional and Western Medicine. *Chin. J. integrated traditional West. Med.* 33 (1), 44–46.

Kitagawa, I., Fukuda, Y., Taniyama, T., and Yoshikawa, M. (1995). Chemical Studies on Crude Drug Processing. X. On the Constituents of Rehmanniae Radix (4) : Comparison of the Constituents of Various Rehmanniae Radixes Originating in China, Korea, and Japan. *Yakugaku Zasshi* 115 (12), 992–1003. doi:10.1248/yakushi1947.115.12_992

Koldkjaer, P., McDonald, M. D., Prior, I., and Berenbrink, M. (2013). Pronounced *In Vivo* Hemoglobin Polymerization in Red Blood Cells of Gulf Toadfish: a General Role for Hemoglobin Aggregation in Vertebrate Hemoparasite Defense? *Am. J. Physiol. Regul. Integr. Comp. Physiol.* 305 (10), R1190–R1199. doi:10.1152/ajpregu.00246.2013

Li, J., Zhang, L. P., Liu, W., Zhang, Z. L., and Liu, L. J. (2005). Studies on the Changes of 5-hydroxymethyl Furfuraldehyde Content in Radix Rehmanniae Steamed for Different Time. *Zhongguo Zhong Yao Za Zhi* 30 (18), 1438–1440. Chinese. PMID: 16381466.

Li, M., Jiang, H., Hao, Y., Du, K., Du, H., Ma, C., et al. (2021). A Systematic Review on Botany, Processing, Application, Phytochemistry and Pharmacological Action of Radix Rehmnniae. *J. ethnopharmacology* 2021, 114820. Advance online publication. doi:10.1016/j.jep.2021.114820

Li, M. M., Wu, L. Y., Zhao, T., Xiong, L., Huang, X., Liu, Z. H., et al. (2011). The Protective Role of 5-HMF against Hypoxic Injury. *Cell Stress Chaperones* 16 (3), 267–273. doi:10.1007/s12192-010-0238-2

Li, P. L., Sun, H. G., Hua, Y. L., Ji, P., Zhang, L., Li, J. X., et al. (2015). Metabolomics Study of Hematopoietic Function of Angelica Sinensis on Blood Deficiency Mice Model. *J. Ethnopharmacol* 166, 261–269. doi:10.1016/j.jep.2015.03.010

Li, X., Dao, M., Lykotrafitis, G., and Karniadakis, G. E. (2017). Biomechanics and Biorheology of Red Blood Cells in Sickle Cell Anemia. *J. Biomech.* 50, 34–41. doi:10.1016/j.jbiomech.2016.11.022

Liu, W., Fan, Y., Tian, C., Jin, Y., Du, S., Zeng, P., et al. (2020). Deciphering the Molecular Targets and Mechanisms of HGWD in the Treatment of Rheumatoid Arthritis via Network Pharmacology and Molecular Docking. *Evid. Based Complement. Alternat Med.* 2020, 7151634. doi:10.1155/2020/7151634

Lucas, A., Ao-Ieong, E. S. Y., Williams, A. T., Jani, V. P., Muller, C. R., Yalcin, O., et al. (2019). Increased Hemoglobin Oxygen Affinity with 5-Hydroxymethylfurfural Supports Cardiac Function during Severe Hypoxia. *Front. Physiol.* 10, 1350. doi:10.3389/fphys.2019.01350

Milano, M., and Schneider, M. (2007). EPO in Cancer Anemia: Benefits and Potential Risks. *Crit. Rev. Oncol. Hematol.* 62 (2), 119–125. doi:10.1016/j.critrevonc.2006.11.011

Pan, L., Li, Z., Wang, Y., Zhang, B., Liu, G., and Liu, J. (2020). Network Pharmacology and Metabolomics Study on the Intervention of Traditional Chinese Medicine Huanglian Decoction in Rats with Type 2 Diabetes Mellitus. *J. Ethnopharmacol* 258, 112842. doi:10.1016/j.jep.2020.112842

Porcu, P., Barron, A. M., Frye, C. A., Walf, A. A., Yang, S. Y., He, X. Y., et al. (2016). Neurosteroidogenesis Today: Novel Targets for Neuroactive Steroid Synthesis and Action and Their Relevance for Translational Research. *J. Neuroendocrinol* 28 (2), 12351. doi:10.1111/jne.12351

Qiang, Y., Liu, J., Dao, M., and Du, E. (2021). *In Vitro* assay for Single-Cell Characterization of Impaired Deformability in Red Blood Cells under Recurrent Episodes of Hypoxia. *Lab. Chip* 21 (18), 3458–3470. doi:10.1039/d1lc00598g

Ru, J., Li, P., Wang, J., Zhou, W., Li, B., Huang, C., et al. (2014). TCMSP: a Database of Systems Pharmacology for Drug Discovery from Herbal Medicines. *J. Cheminform* 6 (1), 13. doi:10.1186/1758-2946-6-13

Sackett, K., Cohn, C. S., Fahey-Ahrndt, K., Smith, A. R., and Johnson, A. D. (2018). Successful Treatment of Pure Red Cell Aplasia Because of ABO Major Mismatched Stem Cell Transplant. *J. Clin. Apher.* 33 (1), 108–112. doi:10.1002/jca.21553

Safeukui, I., Gomez, N. D., Adelani, A. A., Burte, F., Afolabi, N. K., Akondy, R., et al. (2015). Malaria Induces Anemia through CD8+ T Cell-dependent Parasite Clearance and Erythrocyte Removal in the Spleen. *mBio* 6 (1), e02493–14. doi:10.1128/mBio.02493-14

Schiffer, L., Barnard, L., Baranowski, E. S., Gilligan, L. C., Taylor, A. E., Arlt, W., et al. (2019). Human Steroid Biosynthesis, Metabolism and Excretion Are Differentially Reflected by Serum and Urine Steroid Metabolomes: A Comprehensive Review. *J. Steroid Biochem. Mol. Biol.* 194, 105439. doi:10.1016/j.jsbmb.2019.105439

Shi, X., Tang, Y., Zhu, H., Li, W., Li, Z., Li, W., et al. (2014). Comparative Tissue Distribution Profiles of Five Major Bio-Active Components in normal and Blood Deficiency Rats after Oral Administration of Danggui Buxue Decoction by UPLC-TQ/MS. *J. Pharm. Biomed. Anal.* 88, 207–215. doi:10.1016/j.jpba.2013.08.043

Stelzer, G., Rosen, N., Plaschkes, I., Zimmerman, S., Twik, M., Fishilevich, S., et al. (2016). The GeneCards Suite: From Gene Data Mining to Disease Genome Sequence Analyses. *Curr. Protoc. Bioinformatics* 54, 1–33. doi:10.1002/cpbi.5

Wang, X., Shen, Y., Wang, S., Li, S., Zhang, W., Liu, X., et al. (2017). PharmMapper 2017 Update: a Web Server for Potential Drug Target Identification with a Comprehensive Target Pharmacophore Database. *Nucleic Acids Res.* 45, W356–W360. doi:10.1093/nar/gkx374

Wang, Y., Li, C., Chuo, W., Liu, Z., Ouyang, Y., Li, D., et al. (2013). Integrated Proteomic and Metabolomic Analysis Reveals the NADH-Mediated TCA Cycle and Energy Metabolism Disorders Based on a New Model of Chronic Progressive Heart Failure. *Mol. Biosyst.* 9 (12), 3135–3145. doi:10.1039/c3mb70263d

Wishart, D. S., Feunang, Y. D., Guo, A. C., Lo, E. J., Marcu, A., Grant, J. R., et al. (2018). DrugBank 5.0: a Major Update to the DrugBank Database for 2018. *Nucleic Acids Res.* 46 (D1), D1074–D1082. doi:10.1093/nar/gkx1037

Won, T. H., Liao, L., Kang, S. S., and Shin, J. (2014). Simultaneous Analysis of Furfural Metabolites from Rehmanniae Radix Preparata by HPLC-DAD-ESI-MS. *Food Chem.* 142, 107–113. doi:10.1016/j.foodchem.2013.07.026

Wu, Y. S., Chang, C. H., and Nan, F. H. (2016). Steroid Hormone "cortisone" and "20-hydroxyecdysone" Involved in the Non-specific Immune Responses of white Shrimp (Litopenaeus Vannamei). *Fish. Shellfish Immunol.* 56, 272–277. doi:10.1016/j.fsi.2016.07.005

Xia, F., Liu, C., and Wan, J. B. (2020). Characterization of the Cold and Hot Natures of Raw and Processed Rehmanniae Radix by Integrated Metabolomics and Network Pharmacology. *Phytomedicine* 74, 153071. doi:10.1016/j.phymed.2019.153071

Xu, J., Wu, J., Zhu, L. Y., Shen, H., Xu, J. D., Jensen, S. R., et al. (2012). Simultaneous Determination of Iridoid Glycosides, Phenethylalcohol Glycosides and Furfural Derivatives in Rehmanniae Radix by High Performance Liquid Chromatography Coupled with Triple-Quadrupole Mass Spectrometry. *Food Chem.* 135 (4), 2277–2286. doi:10.1016/j.foodchem.2012.07.006

Yao, Z-J., Dong, J., Che, Y-J., Zhu, M-F., Wen, M., Wang, N-N., et al. (2016). TargetNet: a Web Service for Predicting Potential Drug-Target Interaction Profiling via Multi-Target SAR Models. *J. Computer-Aided Mol. Des.* 30, 413. doi:10.1007/s10822-016-9915-2

Yong, W., Chun, L., Wenjing, C., Zhongyang, L., Yulin, O., Dong, L., et al. (2012). Integrated Proteomic and Metabolomic Analysis Reveals Nadh-Mediated Tca Energy Metabolism Disorder in Chronic Progressive Heart Failure. *Heart* 98 (Suppl. 2), E115. doi:10.1136/heartjnl-2012-302920b.12

Zee-Cheng, R. K. (1992). Shi-quan-da-bu-tang (Ten Significant Tonic Decoction), SQT. A Potent Chinese Biological Response Modifier in Cancer

Immunotherapy, Potentiation and Detoxification of Anticancer Drugs. *Methods Find Exp. Clin. Pharmacol.* 14 (9), 725–736.

Zhang, H., Wang, H. F., Liu, Y., Huang, L. J., Wang, Z. F., and Li, Y. (2014). The Haematopoietic Effect of Panax Japonicus on Blood Deficiency Model Mice. *J. Ethnopharmacol* 154 (3), 818–824. doi:10.1016/j.jep.2014.05.008

Zhang, Z., Zhang, Y., Gao, M., Cui, X., Yang, Y., van Duijn, B., et al. (2020). Steamed Panax Notoginseng Attenuates Anemia in Mice with Blood Deficiency Syndrome via Regulating Hematopoietic Factors and JAK-STAT Pathway. *Front. Pharmacol.* 10, 1578. doi:10.3389/fphar.2019.01578

Zhou, Y., Zhou, B., Pache, L., Chang, M., Khodabakhshi, A. H., Tanaseichuk, O., et al. (2019). Metascape Provides a Biologist-Oriented Resource for the Analysis of Systems-Level Datasets. *Nat. Commun.* 10 (1), 1523. doi:10.1038/s41467-019-09234-6

Zhu, M. F., Liu, X. Q., Ju-hee, O., Chang-soo, Y., and Je-Hyun, L. (2007). Zhongguo Zhong Yao Za Zhi = Zhongguo Zhongyao Zazhi = China Journal of Chinese Materia Medica. *China J. Chin. materia Med.* 32 (12), 1155–1157.

Conflict of Interest: The authors declare that the research was conducted in the absence of any commercial or financial relationships that could be construed as a potential conflict of interest.

Publisher's Note: All claims expressed in this article are solely those of the authors and do not necessarily represent those of their affiliated organizations, or those of the publisher, the editors and the reviewers. Any product that may be evaluated in this article, or claim that may be made by its manufacturer, is not guaranteed or endorsed by the publisher.

Copyright © 2022 Zhang, Cui, Su, Wang, Yang, Sun, Guan, Kuang and Wang. This is an open-access article distributed under the terms of the Creative Commons Attribution License (CC BY). The use, distribution or reproduction in other forums is permitted, provided the original author(s) and the copyright owner(s) are credited and that the original publication in this journal is cited, in accordance with accepted academic practice. No use, distribution or reproduction is permitted which does not comply with these terms.